Inorganic Chemistry

Article

pubs.acs.org/IC

A Rapid Microwave-Assisted Solvothermal Approach to Lower-Valent Transition Metal Oxides

Zachary Moorhead-Rosenberg, Katharine L. Harrison, Travis Turner, and Arumugam Manthiram*

Electrochemical Energy Laboratory & Materials Science and Engineering Program The University of Texas at Austin, Austin, Texas 78712, United States

ABSTRACT: A green, rapid microwave-assisted solvothermal process using tetraethylene glycol (TEG) as a reducing agent has been explored as a soft-chemistry route for the preparation of various lower-valent transition metal oxides. To demonstrate the feasibility of the approach, lower-valent binary oxides such as V_4O_9, Mn_3O_4 or MnO, CoO, and Cu_2O have been obtained within a short reaction time of 30 min by reducing, respectively, V_2O_5, MnO_2, Co_3O_4, and CuO with TEG at <300 °C. Moreover, the approach has been used to extract oxygen from ternary oxides such as $LaFeO_3$, $SrMnO_3$, $LaCoO_3$, $LaNiO_3$, and $La_4Ni_3O_{10}$. The oxidation state of the transition metal ions and the oxygen content in these ternary oxides could be tuned by precisely controlling the reaction temperatures from 160 to 300 °C. The products have been characterized by X-ray powder diffraction and iodometric titration. The versatility of this novel technique is demonstrated by the facile synthesis of V_4O_9, which has only been produced recently in single-phase form.

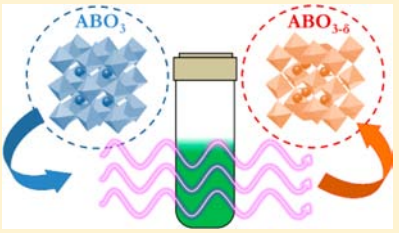

INTRODUCTION

With the recent global interest in renewable energy and energy efficiency, "green" synthesis techniques are being explored in an effort to curb industrial energy usage and waste.[1] Conventional inorganic synthesis procedures, particularly reduction of transition metal oxides to obtain lower-valent oxides, often require high temperatures with long dwell times under hydrogen atmospheres, consuming large amounts of energy. Moreover, these high-temperature procedures are prohibitive to the formation of metastable phases having atypical valence states that may exhibit unique chemical and physical properties of interest to chemists and physicists.[2] With an aim to overcome this limitation, soft-chemistry methods employing borohydride,[2] polyol,[3] sol−gel,[4] and alcohols[5] have been explored to obtain transition metal oxides with reduced valence states. An alternative approach to obtain reduced transition-metal oxides and metal powders is microwave-assisted hydrothermal/solvothermal processing. Utilized extensively in organic syntheses, microwave-assisted techniques offer a variety of advantages over traditional high-temperature methods: lower reaction temperatures, shorter reaction times, and more efficient energy usage.[6−10] The polyol reduction technique has been a popular method to combine with microwave synthesis because of the high boiling point of dihydroxy alcohols and their ability to absorb microwave radiation due to the polar nature of the molecules.[8,9] Microwave irradiation allows the polyol solution to reach the steady-state hold temperature much faster, more efficiently, and more evenly than conventional heating because of the direct dielectric heating and forced convection of the liquid.

While the microwave-assisted polyol method has been investigated as a route to produce transition metal and transition metal oxide nanoparticles (especially those composed of Cu) from solvated metal ion precursors,[8,9,11−15] the reduction of solid transition metal oxide particles in a liquid medium under microwave radiation has not been explored. However, reductions of solid oxides in a liquid medium using conventional heating methods have been studied in the past. For example, one method utilizing a glycerol aqueous solution was employed by Tuysuz et al.[16] to obtain mesoporous CoO from a template Co_3O_4 precursor. This reaction took place over a course of 15 h and required a continuous flow of solution. Another related technique employed NaH as a reducing agent to extract oxygen from $La_4Ni_3O_{10}$ in a heated liquid environment for up to 10 days.[17]

In an effort to decrease the reduction reaction time, we present here a green, ultrafast microwave-assisted method for the reduction of a variety of binary and ternary transition metal oxides using tetraethylene glycol as a reducing agent. Starting with powders of V_2O_5, MnO_2, Co_3O_4, and CuO, we were able to obtain the respective reduced products V_4O_9, Mn_3O_4 or MnO, CoO, and Cu_2O or Cu metal in 30 min at temperatures <300 °C. Additionally, we were able to extract oxygen from powders of $SrMnO_3$, $SrFeO_{3-\delta}$, $LaCoO_3$, $LaNiO_3$, and $La_4Ni_3O_{10}$ by controlling the reaction temperature. The method presented here is a promising, facile way of tuning the oxidation state of metal ions in oxides that may possess interesting variations in physical properties as a function of oxygen content. For example, various rare-earth nickelates such as $RNiO_{3-\delta}$ and $R_2NiO_{4+\delta}$ show changes in resistivity[18,19] and Neèl temperature[20] strongly as a function of oxygen content. Also, the giant magnetoresistance (GMR) effect in $SrFeO_{3-\delta}$ has been reported to be sensitive to the oxygen content value.[21]

Received: July 29, 2013
Published: November 5, 2013

   dx.doi.org/10.1021/ic401943r | Inorg. Chem. 2013, 52, 13087−13093

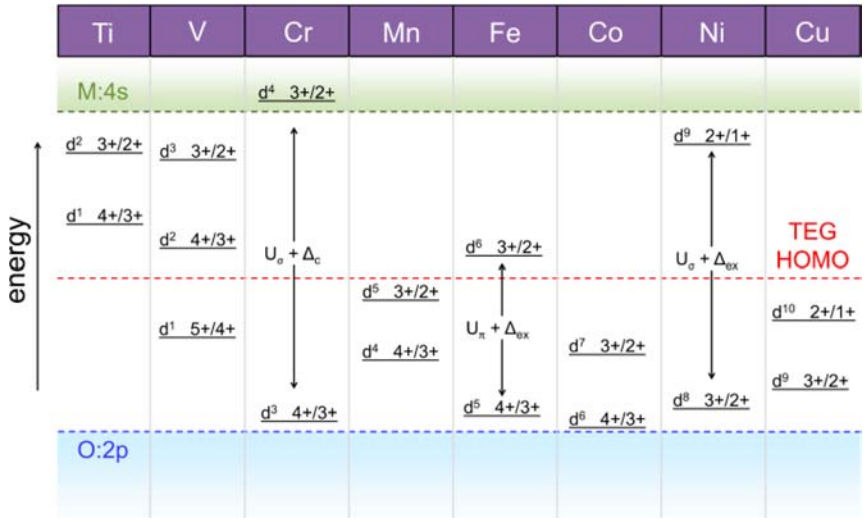

Figure 1. Qualitative redox energies of the 3d transition metal ion couples in octahedral coordination. All oxides with redox couples below the red dotted line are able to be reduced by TEG. U_π and U_σ represent, respectively, the electrostatic potential energy U required to place an electron in a π-bonding t orbital and a σ-bonding e orbital. Δ_c and Δ_{ex} represent, respectively, the crystal field splitting and the intra-atomic exchange interaction associated with electron pairing.

EXPERIMENTAL SECTION

The starting materials V_2O_5, MnO_2, Co_3O_4, and CuO were purchased from Acros Organics (V_2O_5, 98%+), Alfa Aesar (MnO_2, 99.9%), and GFS Chemicals (Co_3O_4, 99.6%; CuO, 99.6%) and used without further purification. $SrMnO_3$, $LaCoO_3$, and $LaNiO_3$ were synthesized by a citrate-based sol−gel method as follows: stoichiometric amounts of $Mn(CH_3COO)_2$, $Co(NO_3)_2{\cdot}6H_2O$, $Ni(NO_3)_2{\cdot}6H_2O$, $La(NO_3)_3{\cdot}6H_2O$ or La_2O_3, and $Sr(NO_3)_2$ were dissolved in a small amount of deionized water and nitric acid with magnetic stirring on a hot plate. Citric acid was added in the ratio of 1:1 for each metal ion, and then ammonium hydroxide solution was poured into the mixture to attain a pH value near 7. For the $SrMnO_3$ reaction, 1 mol of ethylenediaminetetraacetic acid (EDTA) was added per metal ion as a chelating agent in concert with the citric acid. The solution was stirred continuously and heated to ∼95 °C until a gel was formed, at which point the stir bar was removed and the temperature was increased until the gel began to decompose into a powder. The resulting black powder was ground and heated in air at 600 °C for 4 h to remove unwanted carbonaceous products. The resulting powders were then fired at 1000 °C for 24 h, 700 °C for 6 h, and 700 °C for 4 h, respectively, to produce $SrMnO_3$, $LaCoO_3$, and $LaNiO_3$. $SrFeO_{3-\delta}$ was prepared by a previously reported oxalate coprecipitation method by firing at 900 °C for 5 h.[22] $La_4Ni_3O_{10}$ was synthesized by firing a coprecipitated hydroxide−carbonate at 1100 °C for 24 h as reported before.[23]

Reductions of the transition-metal oxides were carried out at various temperatures up to 300 °C for up to 30 min in an Anton-Paar Monowave 3000 microwave synthesis reactor. Specimens consisting of 0.5 g of oxide powder and 10 mL of TEG were enclosed in a thick-walled 30 mL glass vessel and sealed by a hermetic membrane. The mixture was spun at 1200 rpm with a magnetic stir bar to keep the solid particles suspended uniformly in the TEG. Specimens were heated as fast as possible with a maximum power draw of 850 W during initial heating (steady-state power was considerably lower). In all cases, the holding temperature as recorded by an infrared temperature sensor (between 160 and 300 °C) was reached in less than 3 min. The autogenous pressure varied depending on the severity of the reaction conditions; in general, higher temperatures produced higher pressures and the pressure was maintained throughout the hold cycle. Because the boiling point of TEG is above the highest temperature allowed by the microwave (300 °C), the pressure was usually only between 1 and 5 bar. After the 30 min reaction time at the specified temperature (except for the $SrFeO_{3-\delta}$ specimens, which were held for only 10 min), the specimens were cooled to 55 °C and the product was centrifuged to remove the spent TEG. The samples were then washed two times with deionized water and three times with acetone and then dried in air at 100 °C for 20 min.

X-ray diffraction (XRD) patterns were collected with a Rigaku Ultima powder diffractometer utilizing Cu Kα radiation with a 0.02° 2θ step size and a 3 s dwell time. Compositional analysis was accomplished using Rigaku's proprietary software, PDXL, and a whole powder pattern fit (WPPF) technique. PowderCell was used to perform Rietveld refinement of the XRD data of the V_4O_9 sample. SEM images were acquired with a Quanta FEG 650 scanning electron microscope. BET surface area analysis was conducted with a Quantachrome Instruments Autosorb iQ automated gas sorption analyzer. Field-cooled magnetic susceptibility data of V_4O_9 were obtained with a Quantum Design SQUID magnetometer under a field of 1000 Oe as the sample was heated from 5 to 300 K.

Iodometric titration was employed to determine the oxidation state of the metal ions in the ternary oxides $SrMnO_3$, $SrFeO_{3-\delta}$, $LaNiO_3$, and their reduced analogues. Approximately 50 mg of the powder was dissolved by adding 15 mL of 10 wt % KI and 15 mL of 3.5 M HCl, and the solution was titrated against 0.03 M sodium thiosulfate solution, employing starch as the indicator.

RESULTS AND DISCUSSION

Binary Oxides. Binary oxides of the first-row transition series from Ti to Cu were subjected to the microwave solvothermal treatment in TEG, excluding Cr and Ni. Of these oxides, TiO_2 and Fe_2O_3 were not affected by the process, even under the most extreme reaction conditions of 300 °C held for 30 min. The oxides Cr_2O_3 and NiO were not included because Cr^{3+} cannot be reduced to Cr^{2+} in an oxide and the redox potential of $Ni^{2+/+}$ is far too high. As the transition metal 3d electron energies decrease from left to right across the periodic table, the $Ti^{3+/2+}$, $Cr^{3+/2+}$, $Fe^{3+/2+}$, and $Ni^{2+/+}$ redox couples lie above the highest occupied molecular orbital (HOMO) of TEG, whereas the redox couples of $V^{5+/4+}$, $Mn^{4+/3+}$, $Mn^{3+/2+}$, $Co^{3+/2+}$, $Cu^{2+/+}$, and $Cu^{+/(m)}$ lie below the HOMO. Hence, the oxides V_2O_5, MnO_2, Co_3O_4, and CuO are able to be reduced by TEG and TiO_2, Cr_2O_3, Fe_2O_3, and NiO are not.

A qualitative diagram of the transition-metal ion redox energies in octahedral coordination with oxygen is displayed in Figure 1. Ti^{4+} in TiO_2 with a $3d^0$ configuration has no 3d electrons. Because Ti is the first transition element and the

dx.doi.org/10.1021/ic401943r | Inorg. Chem. 2013, 52, 13087−13093

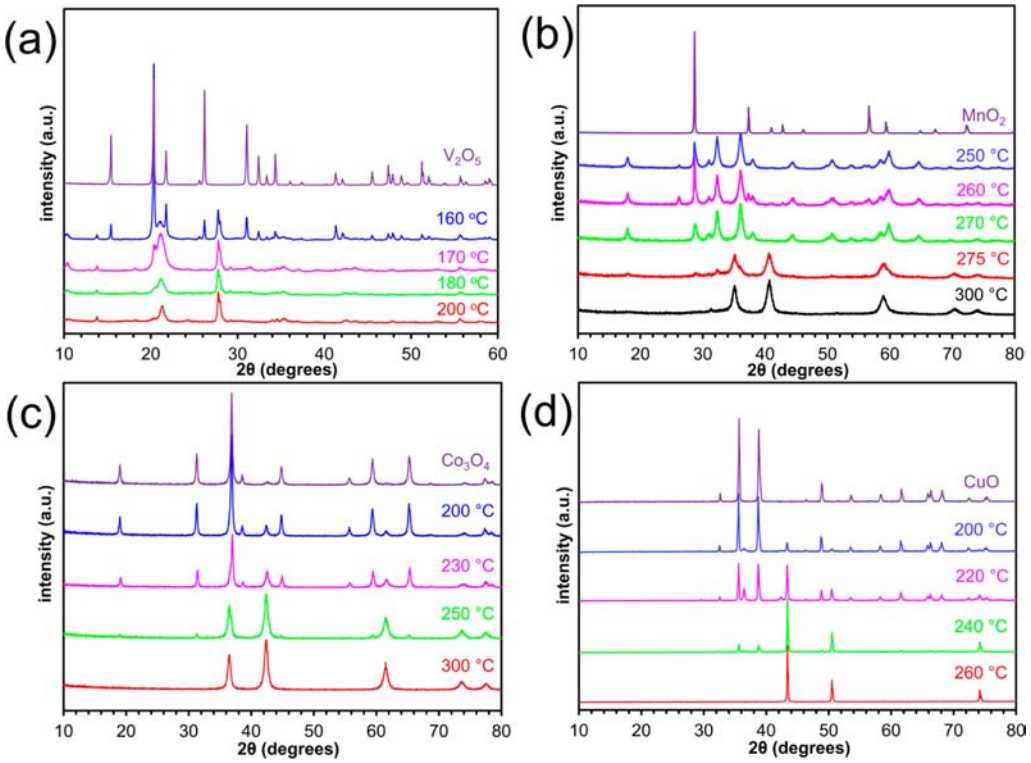

Figure 2. X-ray powder diffraction patterns of (a) V_2O_5, (b) MnO_2, (c) Co_3O_4, (d) CuO and the products formed from each with the microwave-assisted reduction process at the indicated temperatures. In each case, the hold time was 30 min.

intra-atomic exchange stabilization is low, the $Ti^{4+/3+}$ and $Ti^{3+/2+}$ redox couples lie very high in the gap between the full O:2p and empty Ti:4s states. These states are higher than the HOMO of TEG, and so TiO_2 is not reduced. V^{5+} in V_2O_5 also has a $3d^0$ configuration, but the stabilization from the extra proton in the V nucleus pulls the d electron energies down sufficiently that the $V^{5+/4+}$ couple is low enough that TEG can partially reduce V^{5+} to V^{4+}. In Cr_2O_3, the crystal field splitting and electrostatic repulsion term, U_σ, associated with placing an electron in an e orbital which forms a σ bond with oxygen are so high that the $Cr^{3+/2+}$ couple is pushed well above the metal 4s band edge; therefore, Cr^{2+} is not stable. The $Mn^{3+/2+}$ couple is lower than $Cr^{3+/2+}$ because of the higher nuclear charge of Mn and the intra-atomic exchange stabilization associated with a high-spin d^5 state. Because $Mn^{4+}O_2$ is reducible to $Mn^{2+}O$ in TEG, these two stabilizations must be enough to pull the $Mn^{3+/2+}$ couple below the HOMO of TEG. The $Fe^{3+/2+}$ couple is slightly higher than $Mn^{3+/2+}$ due to the intra-atomic exchange associated with adding an electron with opposite spin and is pushed too high for Fe^{3+} to be reduced by TEG. For the same reason, the $Ni^{2+/1+}$ couple is too high; therefore, NiO would remain unaffected during the reaction. Co and Cu are far enough right on the periodic table that their d^7 and d^{10} states, respectively, are sufficiently stabilized as to be lower in energy than the HOMO of TEG.

The XRD patterns of the starting V_2O_5 and the products formed from it are shown in Figure 2a. The reduction of V_2O_5 to the reduced product V_4O_9 was complete within 30 min of microwave irradiation at 180 °C. This is particularly interesting, because V_4O_9 has proven difficult or impossible to synthesize by conventional means and has only recently been obtained and characterized in single-phase form by Yamazaki et al.[24] by a sulfur powder reduction technique.

The ICDD database lists V_4O_9 as a tetragonal phase on the basis of the work of Theòbald et al.[25] However, the peak indexing of our obtained powder pattern to the tetragonal symmetry was unsatisfactory. In addition, the peak at 10.5° could not be accounted for on the basis of tetragonal symmetry. It has been reported previously that V_4O_9 is in fact orthorhombic and not tetragonal, as confirmed by electron diffraction (ED) data.[24,26,27] The orthorhombic *Cmcm* structure proposed by Yamazaki et al.[24] proved to be much more reliable, and all peaks could be indexed on the basis of orthorhombic symmetry. A Rietveld analysis resulted in a satisfactory calculation, as displayed in Figure 3a, with a slightly high R_{wp} value of 16.19% owing to the poor crystallinity of the sample. The lattice parameters reported in this work are compared to previously reported values in Table 1.

To further confirm the formation of V_4O_9, the product obtained from the reduction of V_2O_5 at 200 °C was examined by a SQUID magnetometer. The V^{4+}:$3d^1$ ion in V_4O_9 contains a single unpaired electron; therefore, any reduction of V^{5+} to V^{4+} can be verified by examining the magnetic susceptibility behavior. V_2O_5 with V^{5+}:$3d^0$ ions having no unpaired electrons is diamagnetic. The variation of inverse molar magnetic susceptibility with temperature shown in Figure 3b indicates a linear Curie–Weiss paramagnetic behavior above 150 K with a Curie constant of 0.61. This corresponds to an effective magnetic moment μ_{eff} of 2.21 μ_B, which is close to the theoretical spin-only value of 2.45 μ_B obtained by assuming 2 V^{4+} magnetic centers per formula unit.

X-ray diffraction patterns of MnO_2, Co_3O_4, CuO, and their respective reduced products can be seen respectively in Figure 2b–d. The transformation of MnO_2 (pyrolusite) to MnOOH (manganite), Mn_3O_4 (hausmannite), and finally MnO (manganosite), via microwave-assisted reduction in TEG is detailed

dx.doi.org/10.1021/ic401943r | *Inorg. Chem.* 2013, 52, 13087–13093

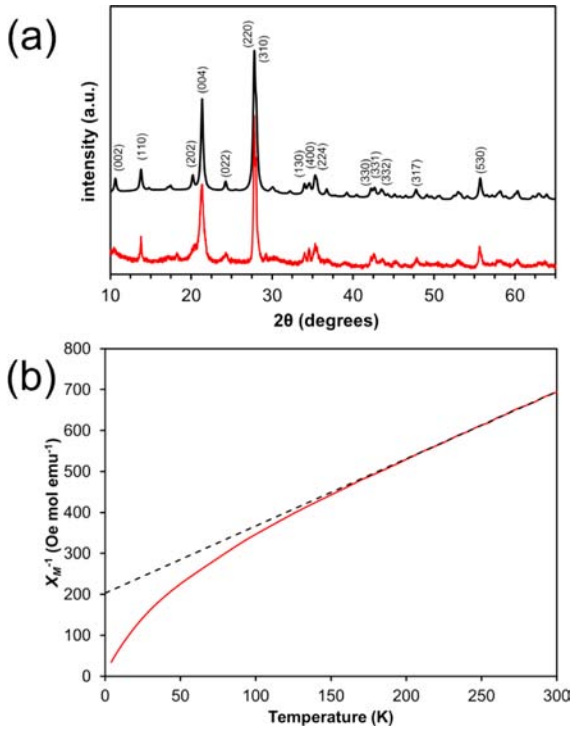

Figure 3. (a) Measured (red, bottom) and calculated (black, top) XRD patterns of V_4O_9 obtained at 200 °C according to the orthorhombic structure outlined by Yamazaki et al.[24] (b) Molar inverse magnetic susceptibility of V_4O_9. The dotted line represents the linear fit to the Curie–Weiss law.

Table 1. Lattice Parameters of V_4O_9

	reference/method			
	Tilley and Hyde[26]/ED	Grymonprez et al.[27]/ED	Yamazaki et al.[24]/XRD	this work/ XRD
a (Å)	8.1	8.235	10.356(2)	10.40(1)
b (Å)	10.4	10.32	8.174(1)	8.13(1)
c (Å)	16.1	16.47	16.559(3)	16.65(1)

Note that *a* and *b* values are reversed for Tilley and Hyde[26] and Grymonprez et al.[27]

in Table 2. After a 270 °C run for 30 min, phase-pure Mn_3O_4 is formed. Likewise, phase-pure MnO can be obtained by microwaving the MnO_2 powder at 300 °C for 30 min. Co_3O_4 forms a cubic spinel structure, with Co^{2+} and Co^{3+} ions respectively occupying the 8a tetrahedral sites and 16d octahedral sites. At reaction temperatures between 200 and 250 °C, the products formed are two-phase mixtures of Co_3O_4 and CoO. However, after 30 min under microwave radiation at 300 °C, pure CoO is formed. Among the 3d transition series oxides, CuO is the only one capable of being reduced to the metallic state by the method presented here. Cu is the last 3d transition metal element and possesses the lowest electron energies; consequently, the Cu oxides are the most easily reduced in TEG (at 300 °C in the microwave reactor, the conversion of CuO to Cu metal occurs in less than 5 min).

SEM images of the binary oxides can be seen in Figure 4. It is interesting to note that the morphologies of the particles remain similar after the microwave reduction. This is because the reduction occurs in the solid state rather than involving a dissolution–recrystallization process. However, some changes are visible, especially in the V and Cu samples, such as an

Table 2. Reduced Binary Oxides Obtained by the Microwave-Assisted Reduction Process for 30 min

starting material	hold temp (°C)	product formed
V_2O_5	180	V_4O_9
V_2O_5	200	V_4O_9
MnO_2	200	MnO_2 (72%), MnO(OH) (28%)
MnO_2	260	MnO_2 (33%), Mn_3O_4 (67%)
MnO_2	270	Mn_3O_4
MnO_2	275	Mn_3O_4 (49%), MnO (51%)
MnO_2	300	MnO
Co_3O_4	200	Co_3O_4 (84%), CoO (16%)
Co_3O_4	230	Co_3O_4 (71%), CoO (29%)
Co_3O_4	250	Co_3O_4 (9%), CoO (91%)
Co_3O_4	300	CoO
CuO	200	CuO (86%), Cu_2O (6%), Cu (8%)
CuO	220	CuO (57%), Cu_2O (15%), Cu (28%)
CuO	240	CuO (30%), Cu_2O (3%), Cu (67%)
CuO	260	Cu

apparent increase in surface roughness. The V_2O_5 to V_4O_9 transformation shows a noticeable change in particle size; the V_4O_9 particles are much smaller and have finer features than the starting material, V_2O_5. During the CuO to Cu transformation, the surface of the material also became much finer. Figure 4h displays some evidence of melting, as small extruded or spherical droplets can be seen. This is expected for small powdered conductive materials, which can absorb microwaves and achieve much higher temperatures than the bulk indicated temperature. Although it is more noticeable in the SEM micrographs of the Cu and V specimens, the surface areas of all samples increased after the microwave reduction process, as revealed by the BET surface area measurements displayed in Table 3.

Ternary Oxides. $SrMnO_3$ adopts a hexagonal 4H hexagonal perovskite structure unless it is slowly cooled from high temperature under an inert atmosphere or rapidly quenched from the high-temperature perovskite phase.[28,29] The $SrMnO_3$ sample prepared for this study under ambient conditions in air had the hexagonal perovskite structure with face-shared octahedra, as indicated by XRD. On the other hand, both $LaNiO_3$ and $SrFeO_{3-\delta}$ had the perovskite structures with corner-shared octahedra. The microwave-assisted solvothermal reductions of $SrMnO_{3-\delta}$, $LaCoO_{3-\delta}$, $LaNiO_{3-\delta}$, and $La_4Ni_3O_{10}$ were carried out at the indicated temperature for 30 min, while those with $SrFeO_{3-\delta}$ were carried out for 10 min since the reduction reaction occurred rapidly with $SrFeO_{3-\delta}$.

According to iodometric titration, the as-prepared $SrMnO_{3-\delta}$, $LaCoO_{3-\delta}$, and $LaNiO_{3-\delta}$ samples are almost fully oxygenated, with oxygen contents close to 3.0 ($\delta < 0.04$). The as-prepared $SrFeO_{3-\delta}$, on the other hand, is oxygen deficient with $\delta = 0.25$. Oxygen content values determined by the redox titration for each compound are given in Table 4.

When these materials are subjected to microwave irradiation in the TEG suspension, topotactic removal of oxygen from the lattice occurs with a concomitant reduction of the transition metal ions. The redox couples present in the ternary oxides investigated here are Mn^{4+}/Mn^{3+}, Fe^{4+}/Fe^{3+}, Co^{3+}/Co^{2+}, and Ni^{3+}/Ni^{2+}. In the case of $SrFeO_{3-\delta}$ and $LaNiO_3$, the transition metals are completely reduced to their 3+ and 2+ oxidation states after being irradiated at 260 °C for 10 min and at 240 °C for 30 min, respectively, to yield $SrFeO_{2.5}$ and $LaNiO_{2.5}$. The

dx.doi.org/10.1021/ic401943r | *Inorg. Chem.* 2013, 52, 13087–13093

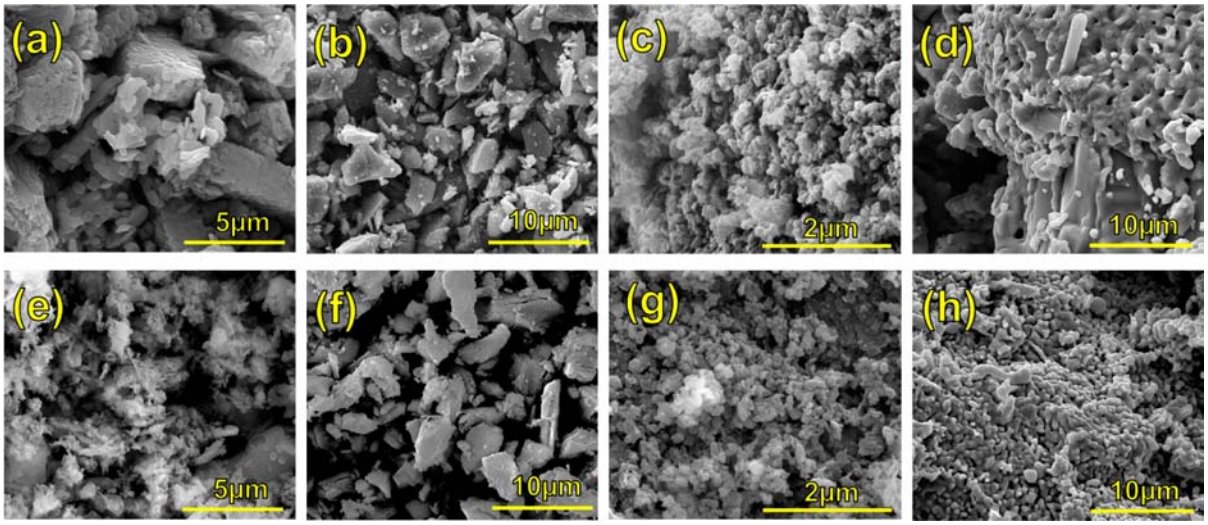

Figure 4. SEM images of the starting binary oxides (a) V_2O_5, (b) MnO_2, (c) Co_3O_4, and (d) CuO and the reduced products (e) V_4O_9, (f) MnO, (g) CoO, and (h) Cu obtained from them under the most extreme microwave conditions given in Table 2.

Table 3. BET Surface Area Measurements

starting material	BET surface area (m^2/g)	product after MW reduction	BET surface area (m^2/g)
V_2O_5	4.096	V_4O_9	9.449
MnO_2	2.121	MnO	18.366
Co_3O_4	23.258	CoO	25.288
CuO	0.332	Cu	4.711
$SrMnO_3$	1.66	$SrMnO_{2.61}$	5.704
$SrFeO_{2.73}$	1.121	$SrFeO_{2.48}$	2.948
$LaCoO_{2.97}$	4.14	$LaCoO_{2.63}$	7.523
$LaNiO_3$	6.268	$LaNiO_{2.53}$	7.203

Table 4. Reduced Ternary Oxides Obtained by the Microwave-Assisted Reduction Process[a]

starting material	hold temp (°C)	oxygen content $(3-\delta)$	oxidation state of the transition metal ion
$SrMnO_{3-\delta}$	as prepared	2.99	3.98
$SrMnO_{3-\delta}$	250	2.71	3.62
$SrMnO_{3-\delta}$	270	2.61	3.21
$SrFeO_{3-\delta}$	as prepared	2.75	3.50
$SrFeO_{3-\delta}$	180	2.73	3.46
$SrFeO_{3-\delta}$	200	2.68	3.36
$SrFeO_{3-\delta}$	220	2.62	3.24
$SrFeO_{3-\delta}$	240	2.56	3.12
$SrFeO_{3-\delta}$	260	2.48	2.95
$LaCoO_{3-\delta}$	as prepared	2.97	2.95
$LaCoO_{3-\delta}$	240	2.86	2.73
$LaCoO_{3-\delta}$	260	2.79	2.57
$LaCoO_{3-\delta}$	280	2.63	2.27
$LaCoO_{3-\delta}$	300	2.63	2.26
$LaNiO_{3-\delta}$	as prepared	3.00	3.00
$LaNiO_{3-\delta}$	200	2.59	2.73
$LaNiO_{3-\delta}$	220	2.76	2.49
$LaNiO_{3-\delta}$	240	2.53	2.06
$LaNiO_{3-\delta}$	260	2.53	2.06
$La_4Ni_3O_{10}$	as prepared	10.0	2.67
$La_4Ni_3O_{10}$	300	9.0	2.0

[a] $SrFeO_{3-\delta}$ samples were held at the indicated temperature for 10 min, while all other reactions were held for 30 min.

XRD patterns detailing the reductions of $SrMnO_{3-\delta}$, $SrFeO_{3-\delta}$, $LaCoO_{3-\delta}$, and $LaNiO_{3-\delta}$ can be seen in Figure 5.

$SrFeO_{2.5}$ is identified as a brownmillerite phase on the basis of the XRD data, while $LaNiO_{2.5}$ is identified as a monoclinic perovskite-like phase with ordered oxygen vacancies and both octahedral and square-coplanar coordinated Ni^{2+} ions. High-spin Fe^{3+} ions with a $3d^5$ configuration in $SrFeO_{2.5}$ have no particular preference for octahedral sites; therefore, the brownmillerite phase with both tetrahedrally and octahedrally coordinated Fe^{3+} ions is formed. Ni^{2+} ions with a $3d^8$ configuration in $LaNiO_{2.5}$, on the other hand, do not prefer tetrahedral coordination; therefore, the reduced Ni ions remain in octahedral coordination or take on square-planar coordination. Compositions with oxygen contents above 2.5 were obtained at temperatures below 300 °C, as shown by the chemical analysis data in Table 4.

According to XRD and titration data (within error), the most reduced phase of $LaCoO_{3-\delta}$ obtained was the intermediate phase $La_3Co_3O_8$ with an average Co oxidation state of +2.33. This product forms as a hybrid of the perovskite and brownmillerite structures with alternating layers of tetrahedrally coordinated Co ions separated by two perovskite layers along the *c* axis.[30]

In the case of $SrMnO_{3-\delta}$, complete reduction of Mn^{4+} to Mn^{3+} was not attainable. At extended dwell times or temperatures higher than 270 °C, the $SrMnO_{3-\delta}$ composition broke down and formed various Sr- and Mn-rich oxides. The lowest achieved oxygen content for $SrMnO_{3-\delta}$ according to the iodometric titration data was 2.63 after irradiation at 270 °C for 30 min, which corresponds to an average Mn oxidation state of +3.26.

SEM images of the ternary oxides can be seen in Figure 6. To a greater extent than in the case of binary oxides, the morphologies of the particles look very similar after reduction, except for the $SrFeO_{3-\delta}$ oxides. The $SrFeO_{3-\delta}$ particles noticeably shrunk in size after the reaction according to the images, similar to the V_2O_5 to V_4O_9 transformation. Because the $SrFeO_{3-\delta}$ to $SrFeO_{2.5}$ reaction occurred quite rapidly in comparison to the others, it is possible that the grains were subjected to rapid strain and crumbled during the reduction process, producing much smaller product grains. In contrast,

dx.doi.org/10.1021/ic401943r | *Inorg. Chem.* 2013, 52, 13087−13093

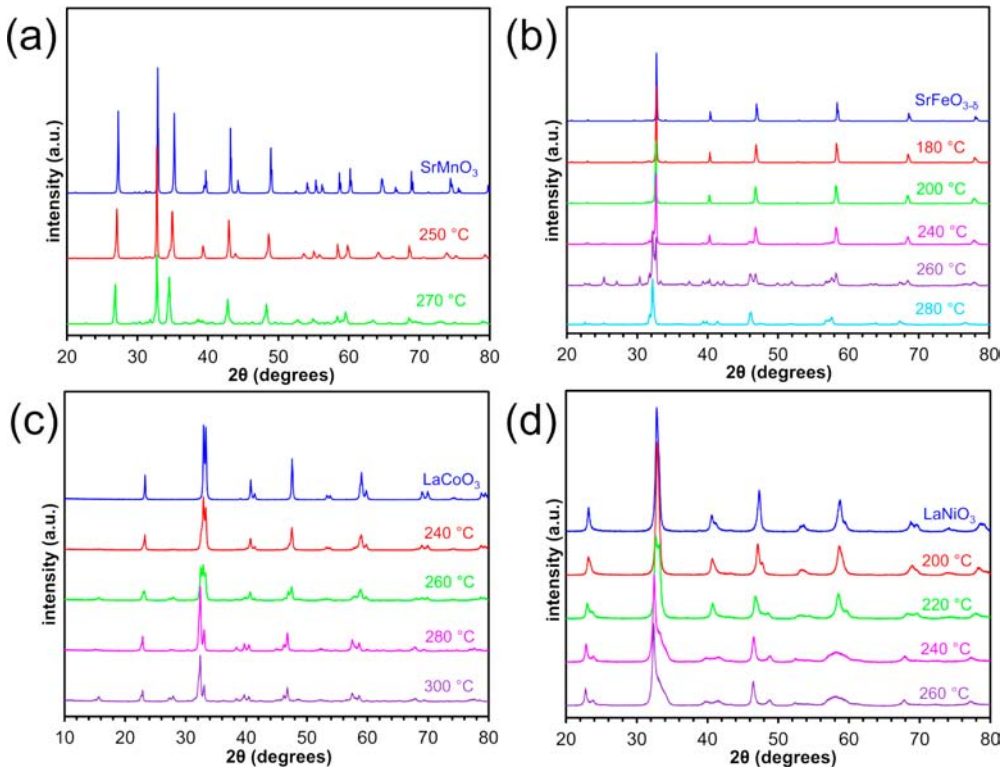

Figure 5. X-ray powder diffraction patterns of (a) $SrMnO_{3-\delta}$, (b) $SrFeO_{3-\delta}$, (c) $LaCoO_{3-\delta}$, (d) $LaNiO_{3-\delta}$ and the products formed from each with the microwave-assisted reduction process at the indicated temperatures. All hold times were 30 min except for the $SrFeO_{3-\delta}$ reduced products, in which case the hold time was 10 min.

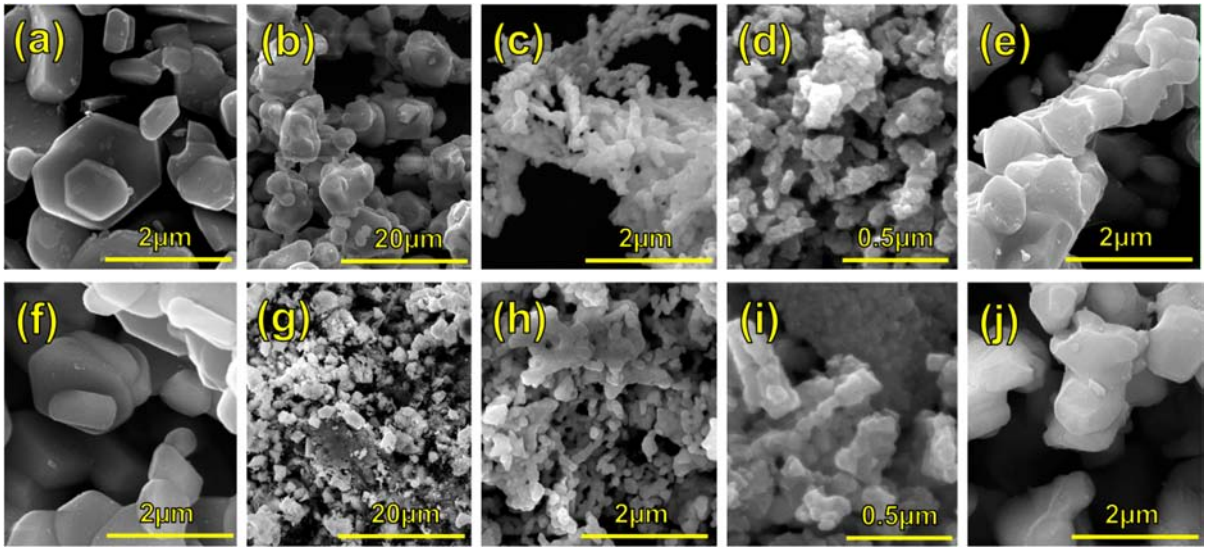

Figure 6. SEM images of the starting ternary oxides (a) $SrMnO_{2.99}$, (b) $SrFeO_{2.73}$, (c) $LaCoO_{2.97}$, (d) $LaNiO_{3.00}$, and (e) $La_4Ni_3O_{10}$ and the final products (f) $SrMnO_{2.61}$, (g) $SrFeO_{2.48}$, (h) $LaCoO_{2.63}$, (i) $LaNiO_{2.53}$, and (j) $La_4Ni_3O_9$ obtained from them under the most extreme conditions given in Table 4.

the Mn-, Co-, and Ni-based perovskites maintained their morphologies after the reduction reaction, although their surface area displayed a notable increase according to the BET analysis (Table 3).

In an effort to demonstrate the applicability of this microwave-assisted solvothermal reduction method to other crystal structures such as those of the Ruddleson−Popper series, $La_4Ni_3O_{10}$ was subjected to the microwave-assisted reduction process at 300 °C for 30 min. Materials of the Ruddleson−Popper series and other structures related to the perovskite family often possess interesting electronic properties that vary considerably with oxygen content; $La_4Ni_3O_{10}$ is one such material.[31] The XRD patterns of $La_4Ni_3O_{10}$ and the reduced product formed from it can be seen in Figure 7. The XRD data reveal that the product formed at 300 °C for 30 min is $La_4Ni_3O_9$ with an oxidation state of 2+ for Ni. A previous synthesis of the $La_4Ni_3O_{10-\delta}$ series involved a more complex electrochemical method to controllably extract oxygen.[31] We

dx.doi.org/10.1021/ic401943r | Inorg. Chem. 2013, 52, 13087−13093

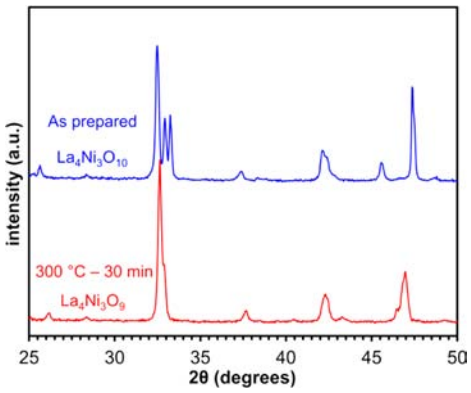

Figure 7. X-ray powder diffraction patterns of as-prepared $La_4Ni_3O_{10}$ and the reduced product, $La_4Ni_3O_9$, after microwave irradiation at 300 °C for 30 min.

have shown here that the microwave-assisted reduction with TEG can quickly produce powdered oxides with easily controllable oxygen content by varying the synthesis temperature. This process will be useful for preparing other metal oxides with variable oxygen content for electronic, magnetic, and chemical studies.

CONCLUSION

In summary, we have developed a facile, microwave-assisted solvothermal technique for the reduction of solid transition-metal oxides utilizing tetraethylene glycol as a reducing agent. The process presented here consumes only a fraction of the time and energy required by conventional high-temperature and alternative soft-chemistry methods. This is particularly enticing, considering the recent interest in green, energy-efficient synthesis procedures. Additionally, this technique provides a quick and highly controllable way to extract oxygen from perovskite and perovskite-like powders with interesting physical properties that vary with oxidation state. Further work is in progress to extend this technique to pelletized and single-crystal specimens so that more precise physical property measurements could be carried out and correlated to oxygen content values.

AUTHOR INFORMATION

Corresponding Author

*E-mail for A.M.: manth@austin.utexas.edu.

Author Contributions

The manuscript was written through contributions of all authors. All authors have given approval to the final version of the manuscript.

Notes

The authors declare no competing financial interest.

ACKNOWLEDGMENTS

This work was supported by the National Science Foundation Materials Interdisciplinary Research Team (MIRT) grant DMR-1122603. We acknowledge Karina Pieratt, Chenxi Zu, and Sheng-Heng Chung for their assistance with the titration analysis, SEM, and BET measurements. We would like to thank Professor John B. Goodenough for fruitful discussion.

REFERENCES

(1) Poliakoff, M.; Fitzpatrick, J. M.; Farren, T. R.; Anastas, P. T. *Science* **2002**, *297*, 807−10.
(2) Manthiram, A.; Dananjay, A.; Zhu, Y. T. *Chem. Mater.* **1994**, *6*, 1601−1602.
(3) Poul, L.; Ammar, S.; Jouini, N.; Fievet, F.; Chimie, L. D. *J. Sol-Gel Sci. Technol.* **2003**, *26*, 261−265.
(4) Chandler, C. D.; Roger, C.; Hampden-smith, M. J. *Chem. Rev.* **1993**, *93*, 1205−1241.
(5) He, W.; Zhang, Y.; Zhang, X.; Wang, H.; Yan, H. *J. Cryst. Growth* **2003**, *252*, 285−288.
(6) Roberts, B. A.; Strauss, C. R. *Acc. Chem. Res.* **2005**, *38*, 653−61.
(7) Kou, J.; Bennett-stamper, C.; Varma, R. S. *ACS Sustainable Chem. Eng.* **2013**, *1*, 810−816.
(8) Bilecka, I.; Niederberger, M. *Nanoscale* **2010**, *2*, 1358−1374.
(9) Polshettiwar, V.; Nadagouda, M. N.; Varma, R. S. *Aust. J. Chem.* **2009**, *62*, 16.
(10) Zhu, X. H.; Hang, Q. M. *Micron* **2012**, *44*, 21−44.
(11) Zhao, Y.; Zhu, J.-J.; Hong, J.-M.; Bian, N.; Chen, H.-Y. *Eur. J. Inorg. Chem.* **2004**, *20*, 4072−4080.
(12) Kawasaki, H.; Kosaka, Y.; Myoujin, Y.; Narushima, T.; Yonezawa, T.; Arakawa, R. *Chem. Commun.* **2011**, *47*, 7740−7742.
(13) Komarneni, S.; Pidugu, R.; Li, Q. H.; Roy, R. *J. Mater. Res.* **2000**, *10*, 1687−1692.
(14) Komarneni, S. *Curr. Sci.* **2003**, *85*, 1730−1734.
(15) Blosi, M.; Albonetti, S.; Dondi, M.; Martelli, C.; Baldi, G. *J. Nanoparticle Res.* **2010**, *13*, 127−138.
(16) Tüysüz, H.; Liu, Y.; Weidenthaler, C.; Schüth, F. *J. Am. Chem. Soc.* **2008**, *130*, 14108−10.
(17) Blakely, C. K.; Bruno, S. R.; Poltavets, V. V. *Inorg. Chem.* **2011**, *50*, 6696−6700.
(18) Xu, X. Q.; Peng, J. L.; Li, Z. Y.; Ju, H. L.; Greene, R. L. *Phys. Rev. B* **1993**, *48*, 1112−1118.
(19) Gayathri, N.; Raychaudhuri, A. K.; Xu, X. Q.; Peng, J. L.; Greene, R. L. *J. Phys: Condensed Matter* **1998**, *10*, 1323−1338.
(20) Gopalan, P.; McElfresh, M. W.; Kakol, Z.; Spalek, J.; Honig, J. M. *Phys. Rev. B* **1992**, *45*, 249−255.
(21) Lebon, A.; Adler, P.; Bernhard, C.; Boris, A. V.; Pimenov, A. V.; Maljuk, A. V.; Lin, C. T.; Ulrich, C.; Keimer, B. *Phys. Rev. Lett.* **2004**, *92*, 037202.
(22) Diodati, S.; Nodari, L.; Natile, M. M.; Russo, U.; Tondello, E.; Lutterotti, L.; Gross, S. *Dalton Trans.* **2012**, *41*, 5517−25.
(23) Manthiram, A.; Tang, J. P.; Manivanan, A. *J. Solid State Chem.* **1999**, *148*, 499−507.
(24) Yamazaki, S.; Li, C.; Ohoyama, K.; Nishi, M.; Ichihara, M.; Ueda, H.; Ueda, Y. *J. Solid State Chem.* **2010**, *183*, 1496−1503.
(25) Thèobald, F.; Cabala, R.; Bernard, J. *C.R. Acad. Sci. Paris, Ser. C* **1969**, *269*, 1209−1212.
(26) Tilley, R. J.; Hyde, B. J. *J. Phys. Chem. Solids* **1970**, *31*, 1613−1619.
(27) Grymonprez, G.; Fiermans, L.; Vennik, J. *Acta Crystallogr.* **1977**, *A33*, 834−837.
(28) Tichy, R. S.; Goodenough, J. B. *Solid State Sci.* **2002**, *4*, 661−664.
(29) Stølen, S.; Bakken, E.; Mohn, C. E. *Phys. Chem. Chem. Phys.* **2006**, *8*, 429−47.
(30) Hansteen, O. H.; Fjellvag, H.; Hauback, B. C. *J. Mater. Chem.* **1998**, *8*, 2081−2088.
(31) Carvalho, M. D.; Cruz, M. M.; Wattiaux, a.; Bassat, J. M.; Costa, F. M. A.; Godinho, M. *J. Appl. Phys.* **2000**, *88*, 544.